Turkish Journal of Remote Sensing, 2025; 7(1); 143-160

Research Article

TURKISH JOURNAL OF REMOTE SENSING
(Türkiye Uzaktan Algılama Dergisi)
e-ISSN 2687-4997
https://dergipark.org.tr/en/pub/tuzal

Can fish kills in Izmir bay be explained with satellite image analysis?

Ahmet Adnan Erdem[1], **Halil Sekerci**[2], **Sebnem Elçi***[3]

[1] *İzmir Institute of Technology, Civil Engineering Department Urla, İzmir, Türkiye; ahmeterdem@iyte.edu.tr; halilsekerci@std.iyte.edu.tr; sebnemelci@iyte.edu.tr*

Check for updates

Article History:
Received: 24 April 2025
Revised: 16 May 2025
Accepted: 20 May 2025
Published: 30 June 2025

Abstract: Motivated by a significant environmental crisis that emerged, where large numbers of dead fish washed ashore in İzmir Bay in the summer of 2024, this study aims to analyze the spatial and temporal dynamics of water quality in the inner bay prior to this incidence. By calculating indices such as NDCI, SABI, and UWQV, and correlating them with climatic data (air temperature, wind speed and relative humidity), this research seeks to document the occurrence and drivers of algal blooms in the bay using Landsat 8 and Sentinel-2 satellite data from 2017 to 2025. This is the first comprehensive study conducted for İzmir Bay that investigates the relationships between water quality indices and climatic variables. It also incorporates aerial analysis of the inner bay to provide a broader spatial perspective. A customized code using Python is developed for this study to independently download and analyze raw satellite data with respect to defined corrections/masks. The results of eight years of analysis indicated that critical conditions arise every summer with air temperatures reaching 40 degrees in the study area. Estimated aerial averaged NDCI index and Chl-a concentration values show a strong positive correlation with air temperature, particularly in the Spearman's rank correlation (rs = 0.67 and 0.62 respectively), indicating a significant relationship between these parameters. Aerial distribution of the indices for the selected critical dates also revealed a significant increase in estimated Chl-a levels during the summer months, specifically in the regions determined from the risk maps produced as a result of this study. The areas with the greatest vulnerability coincide where Poligon, Ilıca streams in the south and Bostanlı and Çiğli streams in the north discharging into the bay. It is recommended that any planned external intervention methods for managing algal blooms should start with these highly vulnerable areas as presented by this study.

Keywords: NDCI; SABI; UWQV; Chl-a; fish kills

Citation: Erdem, A. A., Sekerci, H., & Elçi, Ş. (2025). Can fish kills in Izmir bay be explained with satellite image analysis? *Turk. J. Remote Sens.*, 7(1), 143-160. https://doi.org/10.51489/tuzal.1682454

1. Introduction

Coastal ecosystems are critical environments that provide numerous ecological, economic, and cultural benefits. They provide critical habitats for diverse marine and terrestrial species, support fisheries, and contribute to global biodiversity. These ecosystems act as natural buffers, protecting coastlines from erosion, storms, and flooding. They play a key role in regulating the climate by sequestering carbon in mangroves, salt marshes, and seagrasses. Economically, coastal ecosystems sustain livelihoods through fisheries, tourism, and recreation. They also contribute to food security for millions of people. Additionally, they improve water quality by filtering pollutants and sediments, maintaining the health of marine environments.

However, overpopulated coastal areas are increasingly threatened by anthropogenic pressures and climate change, leading to phenomena such as eutrophication and harmful algal blooms (HABs). Cyanobacterial blooms often occur in eutrophic lakes/lagoons where nutrient inflow is combined with tropical temperatures. Nutrient release can promote excessive algal growth, while temperature changes can alter the composition of toxic cyanobacteria species and their toxins (Beutel & Horne, 2009; El-Shehawy et al., 2012; Häder & Gao, 2015). Excessive growth of cyanobacteria inevitably deteriorates water quality,

*Corresponding Author; Sebnem Elçi / sebnemelci@iyte.edu.tr

causing undesirable taste and odor, reduced oxygen levels in the hypolimnion, and fish and aquatic life mortality due to toxicity. Cyanobacterial proliferation can affect aquatic ecosystems, terrestrial animals, and humans through the food chain. Among cyanotoxins, microcystins are the most common. The World Health Organization (WHO) has set the maximum toxin level in drinking water at 1 μg/L and considers water containing >10^6 cells/mL to be lethal for animals (WHO, 1998). These toxins can reach levels comparable to toxins produced by fungi and plants (Chorus & Welker, 2021). In eutrophic systems like İzmir Bay, excessive nutrient loading combined with warm temperatures can trigger intense cyanobacterial blooms, which rapidly deplete dissolved oxygen—especially at night or during bloom decay—causing hypoxic or anoxic conditions that are lethal to fish. To control and manage the excessive growth of cyanobacteria and other phytoplankton, restricting nutrient inputs is necessary. Effective long-term control of harmful microalgae typically requires reducing both nitrogen and phosphorus inputs. In some cases, nutrient reduction alone may not suffice, and alternative methods such as artificial mixing can be employed. İzmir Bay, located on the western coast of Turkey, is a prime example of a semi-enclosed coastal ecosystem that has experienced significant ecological changes over the past few decades due to urbanization, industrial activities, and agricultural runoff. While previous studies have examined local water quality and algal bloom events in the bay, many of these studies have been limited to point-based measurements or short-term observations. This study fills a critical gap by utilizing satellite-based remote sensing data, which offers comprehensive, high-resolution spatial and temporal coverage over a longer time frame (2017–2025). By combining satellite data with climatic factors, this research will provide a more detailed understanding of the dynamics of algal blooms and water quality in İzmir Bay, allowing for a more robust analysis of their causes and long-term trends

Recently (on August 20, 2024), a significant environmental crisis emerged in the İzmir Bay. Large numbers of dead fish washed ashore, accompanied by a strong foul odor (Figure 1). The incident was linked to two main factors: pollution from untreated domestic and industrial wastewater, and elevated sea surface temperatures. These conditions promoted excessive algal growth and resulted in oxygen depletion, ultimately creating an inhospitable environment for marine life. These conditions created a hostile environment for marine life, leading to the observed fish deaths. İzmir Bay, as a highly populated and economically vital region, plays a key role in regional fisheries, tourism, and urban sustainability. Its ecological degradation has direct implications for public health, biodiversity, and the local economy. While specific toxin measurements for İzmir Bay remain limited, recent reports from local monitoring agencies have highlighted increasing chlorophyll-a levels and low dissolved oxygen concentrations during summer months—conditions favorable for cyanobacterial dominance and potential toxin release. These trends suggest a growing risk of microcystin contamination in the bay, warranting further investigation. In recent years, increasing algal blooms and dissolved oxygen deficiencies in the Gulf of Izmir indicate serious problems with water quality. Fish deaths, especially in the summer months, have been documented by scientific and local observations (TMMOB, 2024). Aktaş et al. (2022) showed in their measurements at different points of the Gulf that nutrient accumulation and oxygen deficiency negatively affect the ecosystem, especially during hot periods, and accelerate the eutrophication process. In a news report shared by Anadolu Agency (2024), it was reported that fish deaths continued even as of January, and that citizens observed foul odors and clusters of dead fish on the sea surface. Such scientific and visual observations reveal both seasonal and ecological effects of water quality deterioration in the region; and support the importance of remote sensing-based analyses used in this study. Motivated partly by this incident, this study aims to analyze the spatial and temporal dynamics of water quality in the inner region of İzmir Bay from 2017 to 2025 using Landsat 8 and Sentinel-2 satellite data. By calculating indices such as NDCI, SABI, and UWQV, estimating Chl-a concentrations and correlating them with climatic data, this research seeks to document the occurrence and driving forces of algal blooms in the bay. The study provides a novel integration of satellite-based analysis and environmental variables, offering insights that can support early warning system and inform effective management strategies for the bay.

Figure 1. Fish kills observed in the inner section of Izmir Bay in August, 2024 (Anadolu Agency, 2024)

2. Study site

The study was conducted in the inner section of İzmir Bay (Figure 2), a semi-enclosed water body located along the Aegean Sea in western Türkiye. The bay, crescent-shaped and spanning approximately 50 km in length and 15–20 km in width, supports diverse marine life and wetland habitats, including migratory birds in nearby areas such as the Gediz Delta. Geographically, it is divided into three sections: Outer, Middle, and Inner Bay Areas.

The inner bay, which suffers from limited water circulation and its proximity to urban and industrial zones, is the most polluted area. Rapid urbanization in İzmir has led to heavy contamination from domestic, industrial, and agricultural waste, resulting in issues such as eutrophication, sedimentation, and periodic fish kills. Pollution is primarily driven by the discharge of untreated sewage and industrial effluents through drainage systems. Major industries in İzmir, including food processing, beverage production, chemical manufacturing, paper production, textiles, and metal processing, are concentrated in coastal and basin areas, contributing significantly to elevated levels of heavy metals and other pollutants. The restricted water exchange in the inner bay further amplifies these environmental challenges.

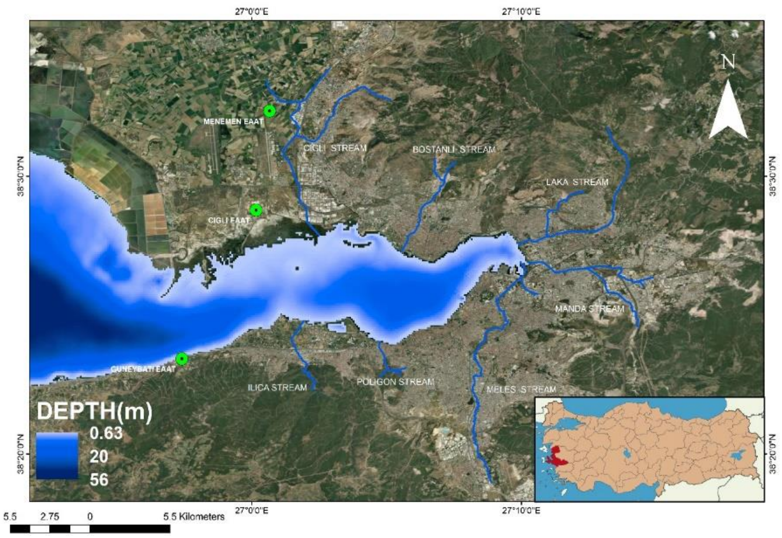

Figure 2. Map of Izmir bay showing bathymetry of the inner bay and the seven streams discharging into the bay (The water treatment plants discharging into the bay are also shown by green circles)

Based on the water quality values monitored by the ministry in the inner bay of Izmir, TRIX index values were calculated between 2016 and 2022 by the Turkish Ministry of Environment, Urbanization and Climate (Aegean Sea Water Quality Report, 2022). TRIX index combines pressure variables (nutrients) and response variables (oxygen and Chl-a) related to eutrophication and Index values above 6 indicate a very high trophic level (severe eutrophication), while values above 4 reflect a high trophic level. As can be seen in Figure 3, the inner bay stayed above the high trophic level in most of the summers during the monitoring program. Monitored chlorophyll concentrations reached to 40 µg/l in years 2018 and 2021.

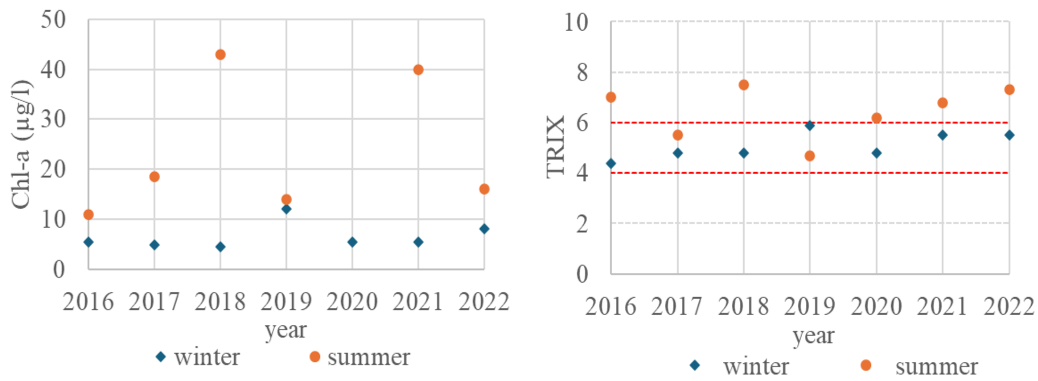

Figure 3. (a) Monitored Chlorophyll-a concentrations and (b) estimated TRIX values for the inner bay of Izmir (adopted from Aegean Sea Water Quality Report, 2022)

Despite years of scientific and technical studies and the efforts of relevant institutions to address pollution in İzmir Bay, desired results have not been achieved, and the pollution in the bay has increased. The following common findings were stated that the bay is under a heavy pollution load and pollution is entering the bay from various sources. Seven streams discharging into the inner bay (Ilıca, Poligon, Meles, Laka, Manda, Bostanlı and Çigli streams) carry a significant organic pollution load. Domestic, industrial, and agricultural waste flows into the inner Bay via streams throughout the year, with an increase during rainy periods.

2.1. Climatic conditions in the study area

The climate of İzmir is classified as Mediterranean, with hot, dry summers and mild, wet winters. Due to its coastal location, the city experiences moderate temperatures throughout the year, with summer highs often reaching above 30°C and winter lows rarely falling below 5°C. Precipitation is mainly concentrated in the winter months, while the summer season is typically dry, making it a popular destination for tourists seeking sunny weather. Climatic variables, such as temperature, wind speed, and humidity, play a crucial role in the formation of algal blooms and fish kills in the study area. Higher temperatures, especially in summer, accelerate the metabolic processes of algae, promoting rapid growth and the potential for cyanobacterial blooms, which can lead to oxygen depletion in the water. Wind speed can influence the mixing of water layers, which may either exacerbate or alleviate bloom formation by affecting the distribution of nutrients and algae. Additionally, variations in humidity can affect the evaporation rates and water salinity, further influencing the likelihood of eutrophic conditions. Throughout the data analysis period, the average temperature was 25°C, with a maximum recorded value of 40°C; the average wind speed was 4.3 m/s, with a maximum recorded value of 10.5 m/s; and the average relative humidity was 63%, with a maximum recorded value of 91%. These climatic conditions suggest that high summer temperatures and low wind speeds may promote favorable conditions for algal bloom formation and increase the risk of hypoxic conditions, potentially contributing to fish kills in the inner bay (Figure 4).

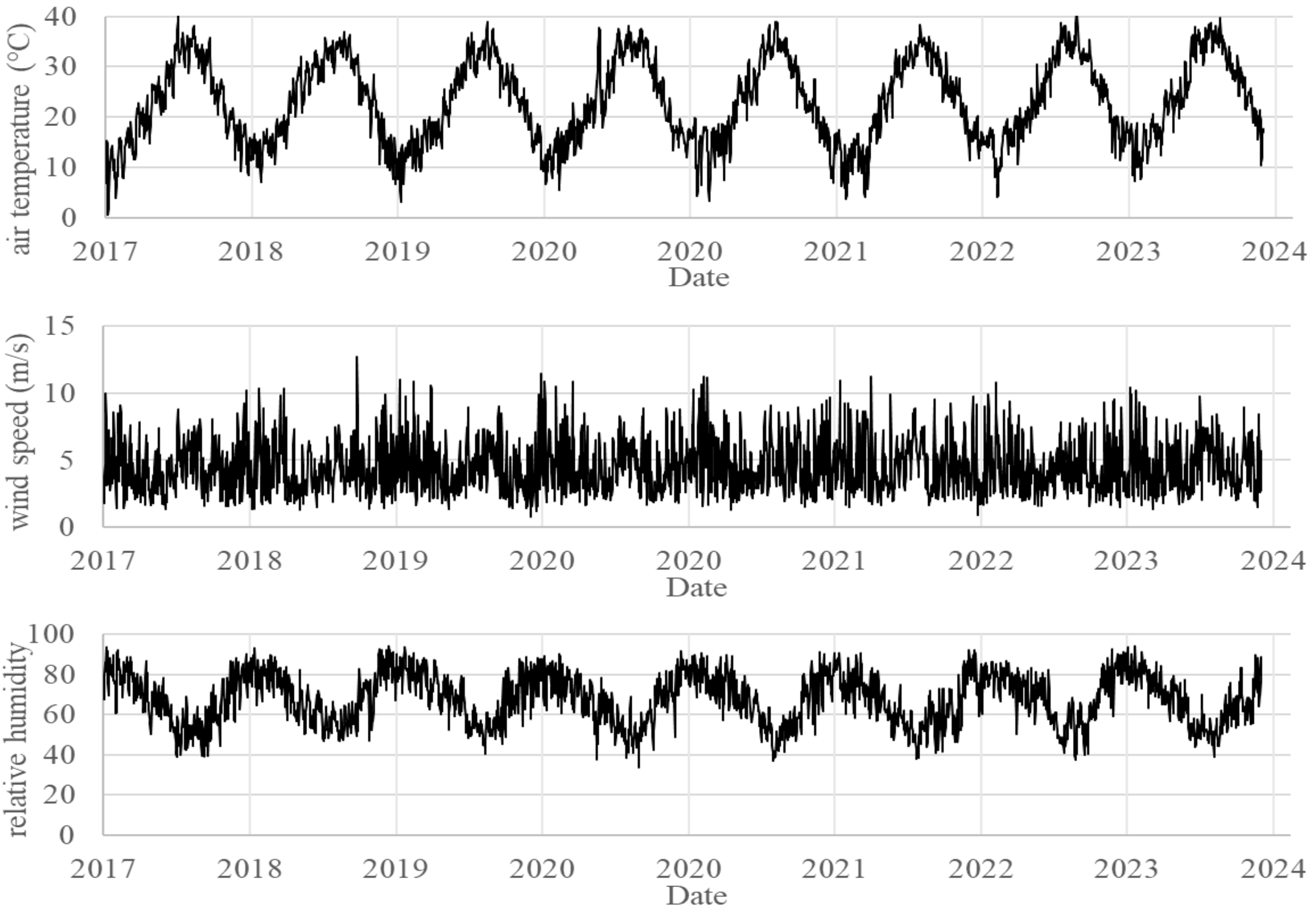

Figure 4. Time series of observed climatic factors in the inner bay of Izmir

3. Remote Sensing for Analyzing Coastal and Marine Environments

Remote sensing has emerged as an indispensable tool for monitoring and analyzing coastal and marine environments. Satellite imagery from platforms like Landsat 8 and Sentinel-2 offers high-resolution, multispectral data, enabling the calculation of indices that can be used to assess water quality and detect algal blooms. Indices such as the Normalized Difference Chlorophyll Index (NDCI), the Surface Algal Bloom Index (SABI), and the Ulyssys Water Quality Viewer (UWQV) provide critical insights into the spatial and temporal dynamics of water quality parameters, including chlorophyll-a concentrations and suspended particulate matter.

Remote sensing enables accurate estimation of chlorophyll-a concentrations in aquatic ecosystems (Ndungu et al., 2013). This method significantly reduces problems associated with missing data (undersampling), as it provides temporal and large-scale data for the desired duration of the study with reduced costs and significant savings in data collection efforts (Chawira et al., 2013; Ndungu et al., 2013). Using remote sensing, surface reflectance from the water body is measured to determine chlorophyll-a concentration, dissolved organic matter, or total suspended solids (TSS) (Han & Rundquist, 1997; Gitelson et al., 2009; Chawira et al., 2013; Ndungu et al., 2013). Among the many advantages of remote sensing is its ability to facilitate the improvement and testing of biological models for a large area coverage employing systematic data collection, which can eliminate sampling bias and prepare large datasets for analysis (Han & Rundquist, 1997; Thiemann & Kaufmann, 2002).

A number of previous studies have demonstrated the effectiveness of satellite-based remote sensing for monitoring and assessment of water quality in inland and coastal environments and highlighted the utility of satellite data for deriving chlorophyll-a concentrations, which are key indicators of phytoplankton biomass and potential eutrophication (Mishra & Mishra, 2012; Zhang et al., 2020; Davis et al., 2019; SSEC, 2012). The previous studies highlight the effectiveness of the water quality indices primarily NDCI and SABI in estimating chlorophyll-a concentrations across various aquatic environments. Mishra & Mishra (2012) demonstrated NDCI's reliability in turbid waters and SABI's superior performance in detecting floating algal blooms. Zhang et al. (2020) emphasized the benefits of combining SABI with other indices to enhance accuracy in complex water systems. Davis et al. (2019) demonstrated SABI's ability to outperform traditional algorithms in moderate turbidity environments. The findings across these studies highlight the potential of these indices to improve water quality monitoring, particularly in environments with variable turbidity and spectral complexities. However, these studies did not investigate the relation of indices to climatic factors or explore variations across broader spatial areas. They typically calculated variations at single prefined points, whereas our analysis considers entire inner bay area considered for this study and averages cell values to derive a single representative value for the studied area. This approach offers a more comprehensive understanding of spatial and temporal dynamics in algal bloom monitoring.

The occurrence and intensity of algal blooms are closely linked to climatic factors such as sea surface temperature (SST), precipitation, and wind patterns. A study by Paerl & Huisman (2008) have shown that warmer temperatures and altered precipitation regimes due to climate change exacerbate eutrophication and algal blooms. The findings reveal that NDVI was positively correlated with precipitation, humidity, temperature, and sunshine hours, while negatively correlated with atmospheric pressure. Climatic factors emerged as the dominant drivers of NDVI variations across land types, including croplands, forests, and grasslands, highlighting their critical role in shaping vegetation dynamics.

Alharbi (2023) used spectral indices (quantitative measurements derived from satellite reflectance data to assess surface characteristics) such as Chlorophyll a (Chl-a) and Surface Scum Index (SSI), to monitor algal bloom dynamics in the area between Jeddah and Rabigh on the Red Sea Coast. The findings highlight that factor influencing algal blooms included surface water temperature (inverse correlation), wind speed (direct correlation), and proximity to estuaries, which were identified as prime zones for bloom proliferation. However, their study considered a very limited temporal analysis (with less than one year of data). Tuygun et al. (2023) investigated Lake Burdur, Turkey, which faces environmental challenges such as nutrient influx from diffuse sources and anthropogenic stress using Google Earth Engine (GEE) to analyze chlorophyll-a (Chl-a) concentrations and calculate the Trophic State Index (TSI) to understand the lake's eutrophication trends. In the literature, many studies (i.e., Alharbi, 2023; Tuygun et al, 2023) utilizing Google GEE for atmospheric corrections and satellite data analysis are available. For the purposes of this study, we developed a customized code using Python to independently download and analyze raw satellite data with respect to defined corrections/masks (available as Data Supplement). This approach provides greater flexibility and control over data processing, ensuring robust and tailored insights into water quality and algal bloom dynamics.

3.1. Landsat 8 and Sentinel-2 data

Landsat 8 is a satellite launched by the United States Geological Survey (USGS) and NASA as part of the Landsat program on February 11, 2013. It features with two main instruments: the Operational Land Imager (OLI) and the Thermal Infrared Sensor (TIRS). The OLI sensor captures images in the visible, near-infrared (NIR), and shortwave infrared (SWIR) ranges across nine spectral bands, while the TIRS sensor provides thermal imagery using two thermal infrared bands. Landsat 8 has a 16-day revisit cycle and offers global coverage.

Sentinel-2 is a satellite launched under the European Union’s Copernicus Programme. The specific satellite used in this study is Sentinel-2B, which was launched on March 7, 2017, and is the second satellite in the Sentinel-2 series. It is equipped with the Multispectral Instrument (MSI), which captures imagery across 13 spectral bands, covering visible, near-infrared (NIR), and shortwave infrared (SWIR) wavelengths. The spatial resolution varies between 10, 20, and 60 meters depending on the spectral band. The combined Sentinel-2 series has a 5-day revisit time, enabling frequent Earth monitoring. For this study, only atmospherically corrected Sentinel-2B Level-2A (L2A) data is used, with two datasets per month selected.

The complementary features of Landsat 8 and Sentinel-2 data provide researchers with the opportunity to harness the strengths of both platforms. Landsat 8's thermal bands are particularly useful for temperature-related studies, while Sentinel-2's higher spatial resolution and more frequent revisit intervals improve the detection of localized and dynamic changes in water quality (Table 1). Combining these datasets enables a more comprehensive analysis of coastal ecosystems, allowing researchers to address both long-term trends and short-term episodic events.

Table 1. Comparison of spectral and spatial details on Landsat-8 and Sentinel-2 satellites

Landsat 8 operational land imager (OLI) and Thermal Infrared Sensor (TIRS) launched February 11, 2013			Sentinel-2 Multispectral instrument (MSI) launched March 7, 2017 (Sentinel-2B)		
Bands	**Wavelength (µm)**	**Resolution (m)**	**Bands**	**Wavelength (µm)**	**Resolution (m)**
Band 1 - Coastal Aerosol	0.43-0.45	30	Band 1 - Coastal Aerosol	0.443	60
Band 2 - Blue	0.45-0.51	30	Band 2 - Blue	0.458 - 0.523	10
Band 3 - Green	0.53-0.59	30	Band 3 - Green	0.543 - 0.578	10
Band 4 - Red	0.64-0.67	30	Band 4 - Red	0.650 - 0.680	10
Band 5 - Near Infrared	0.85-0.88	30	Band 5 - Vegetation Red Edge	0.698 - 0.713	20
Band 6 - SWIR 1	1.57-1.65	30	Band 6 - Vegetation Red Edge	0.733 - 0.748	20
Band 7 - SWIR 2	2.11-2.29	30	Band 7 - Vegetation Red Edge	0.773 - 0.793	20
Band 8 - Panchromatic	0.5-0.68	15	Band 8 - NIR	0.785 - 0.899	10
Band 9 - Cirrus	1.36-1.38	30	Band 8A - Vegetation Red Edge	0.865	20
Band 10 - Thermal infrared (TIRS) 1	10.6-11.19	100	Band 9 - Water Vapour	0.945	60
Band 11 - Thermal infrared (TIRS) 2	11.50-12.51	100	Band 10 - SWIR - Cirrus	1.375	60
			Band 11 - SWIR	1.610	20
			Band 12 - SWIR	2.190	20

3.2. Water quality Indices for algal bloom detection

The integration of remote sensing into water quality monitoring has proven invaluable for providing wide coverage, high temporal resolution, and detailed data on key water quality parameters. While traditional water sampling methods are time-consuming and costly, remote sensing (RS) technologies, particularly cloud-based platforms like Google Earth Engine (GEE), enable efficient spatial and temporal analyses. Recent advancements in the field promise to further enhance its utility. Innovations such as enhanced sensor capabilities offer higher resolution, broader spectral ranges, and improved accuracy, enabling more precise monitoring. Physics-based algorithms have also improved data confidence by incorporating corrections for atmospheric and water column properties, standardizing data across different satellites, and refining parameter extraction.

The development of spectral indices tailored for aquatic environments has significantly advanced the detection and monitoring of algal blooms. The NDCI (Normalized Difference Chlorophyll Index), as proposed by Mishra & Mishra (2012), has been widely used to quantify chlorophyll-a concentrations, especially in eutrophic waters. SABI (Surface Algal Bloom Index), introduced by Alawadi (2010), is a promising index for assessing submerged aquatic vegetation and its responses to environmental stressors. Meanwhile, UWQV (Ulyssys Water

Quality Viewer), developed by Zlinszky & Padányi-Gulyás (2020), leverages the ultraviolet region of the electromagnetic spectrum to assess water quality variables such as dissolved organic matter (DOM) and turbidity.

NDCI is a spectral index developed to estimate chlorophyll-a concentrations, particularly in turbid and productive waters. It uses satellite data to measure the difference in reflectance between the vegetation red-edge (VRE) and red spectral bands, which are sensitive to chlorophyll content (Equation 1). It is commonly used in remote sensing to assess water quality, predict algal bloom occurrence, and study the correlations between chlorophyll-a levels and environmental factors.

$$NDCI = \frac{\mathrm{VRE} - \mathrm{Red}}{\mathrm{VRE} + \mathrm{Red}} \tag{1}$$

ABI is designed to detect and monitor surface algal blooms, including floating microalgae like cyanobacteria. It leverages the unique spectral properties of algal blooms, particularly their reflectance in the near-infrared (NIR), blue and green bands those are primarily sensitive to green plants, pure water and algal blooms respectively (Equation 2). SABI can differentiate floating algae from clear blue waters and/or blooms mixed with green planktonic waters. Negative SABI values indicate the buoyancy state of algae relative to their photosynthetic activity. This suggests that the species may be located deeper in the water column, where high water absorption occurs in the NIR.

$$SABI = \frac{\mathrm{VRE} - Red}{Blue + Green} \tag{2}$$

UWQV is a custom script designed for analyzing chlorophyll-a and sediment concentrations in coastal and inland waters. It incorporates multiple indices, including MCI (Maximum Chlorophyll Index) (Equation 3), TSS (Total Suspended Sediment) (Equation 4), and NDWI (Normalized Difference Water Index) (Equation 5), to create a weighted average that identifies clean water, sediment-filled areas, and regions with high chlorophyll concentrations. The UWQV algorithm utilizes a step-by-step process where snow, cloud, and shadow pixels are masked, followed by the visualization of chlorophyll and sediment concentrations. Chlorophyll is displayed where sediment levels are low, while sediment concentrations are layered transparently in medium cases or dominate the visualization when high. Water masking is performed using the Normalized Differential Water Index (McFeeters, 1996). Cloud masking is carried out using either the Hollstein et al. (2016) method or the Braaten-Cohen-Yang cloud detector (Braaten et al., 2015). Chlorophyll estimation relies on reflectance-based indices, such as MCI, depending on the spectral capabilities of the satellite.

$$MCI = \mathrm{VRE} - \left(\frac{0.74 - 0.705}{0.74 - 0.665}\right) * Red - \left(1 - \frac{0.74 - 0.705}{0.74 - 0.665}\right) * \mathrm{VRE} \tag{3}$$

$$TSS = \mathrm{VRE} \tag{4}$$

$$NDWI = \frac{Green - NIR}{Green + NIR} \tag{5}$$

3.3. Chlorophyll-a (Chl-a) analysis

Chlorophyll-a is a pigment found in photosynthetic organisms, commonly used as a proxy for algal biomass in water quality studies. Remote sensing indices like NDCI, FLH (Fluorescence Line Height), and MCI help quantify chlorophyll-a concentrations in aquatic environments. These indices are instrumental in tracking algal blooms, understanding eutrophication processes, and monitoring ecosystem health. Chlorophyll-a (Chl-a) is a crucial parameter for assessing eutrophication by measuring algae density. The satellites capture reflectance data across specific wavelengths of light (visible, infrared, etc.), which are affected by the presence of Chl-a in water. For example: Blue light (short wavelength) is absorbed by Chl-a.Red and near-infrared light are reflected by water with high algal content. Following the previous studies (Hansen & Williams, 2018; Tuygun et al., 2023), we applied empirical equations (mathematical models that relate reflectance values to known Chl-a concentrations), to the inner bay area to estimate Chl-a levels from satellite images (Equation 6).

$$Chla = e^{\left(1.64-1.58*\log(NIR)-1.69*\frac{Green}{Red}-0.28*\frac{Green}{SWIR}+1.28*\log(Green)\right)} \tag{6}$$

3.4. The trophic state index (TSI)

TSI is a classification system used to describe the trophic status of a water body based on its productivity, nutrient levels, and clarity. Developed by Carlson (1977), it is widely applied to lakes and reservoirs to assess eutrophication levels. The TSI provides insights into ecological health, water quality, and nutrient management, making it a critical tool for understanding and mitigating eutrophication. TSI values can be classified into three levels: oligotrophic (TSI<30), mesotrophic (30<TSI<50), and eutrophic (TSI>50). The eutrophic status states high to excessive productivity, often associated with algal blooms and poor water quality The TSI equation associated with Chl-a concentration in mg/m^3 was applied in this study. (Equation 7):

$$TSI = 9.81 \times \ln(Chl - a) + 30.6 \tag{7}$$

The integration of NDCI, SABI, and UWQV indices and prediction of Chl-a allows for detailed analysis of algal blooms in the bay. By combining these indices with climatic data such as air temperature, relative humidity, and wind patterns, researchers can identify key drivers of algal blooms and their impacts on water quality and coastal ecosystems. This study also focused on specific dates which stood out as problematic days on the time series of indices calculated from the available satellite data. Spatial variation of both the indices and the Chl-a concentrations are plotted on those specific dates and risk maps for the inner bay are produced by overlaying the spatial maps for the critical conditions.

4. Methodology

This study aims to analyze the spatial and temporal dynamics of water quality in the inner İzmir Bay from 2017 to 2025 using Landsat 8 and Sentinel-2 satellite data. By calculating indices such as NDCI, SABI, and UWQV, and correlating them with climatic data, this research seeks to document the occurrence and drivers of algal blooms in the bay.

For the study area, understanding the interplay between climatic drivers and water quality indices is essential for developing effective management strategies. The applied methodology is non-invasive and allows researchers to monitor the study area at a large scale and high temporal resolution without needing continuous field measurements (Figure 5). It also provides insights into how human activities and climatic factors have influenced İzmir Bay’s eutrophication trends over time.

All analyses conducted in this study were performed using original, customized scripts developed specifically for this research (available as Data Supplement). The codes were designed to calculate water quality indices, such as NDCI, SABI, UWQV, and to estimate Chl-a concentrations, using Sentinel-2 and Landsat-8 satellite imagery within a specific study area. Python was used for this study and Sentinel library was established. Sentinel Hub browser is connected with a "CLIENT ID" and a "Configuration Utility" is created according to the type of satellite used. Data is taken every day between specific dates (Delta days), but must be provided under specific conditions. Data is customized with specified boundary conditions;

these are cloud mask (maxCloudCoverage) and data pixel dimensions. For a specific area ("type": "Polygon"), the bands obtained from satellites are arranged according to the evalscript of the analysis. Two bands are used for NDCI (Normalized Difference Chlorophyll Index), they are "red" and "vegetation red edge". These bands are processed as a single index to obtain an output file as a single band. For SABI (Soil Adjusted Vegetation Index), an index consisting of 4 different bands is created and a single band is obtained (Red, Blue, Green, NIR). For CHL-a, 4 different bands are converted to a single band file (Red, Green, Vegetation red edge, SWIR). UWQV is the weighted average of three different analyses with many components. During this cycle, the average of all pixels in this area is printed as a "CSV" file for each day that meets the condition. The obtained satellite images are saved as a "TIFF" file. Meteorological data for statistical studies were provided by the "CERES" satellite. The data received for all dates were arranged for dates that provide boundary conditions to match the water quality indices. In this way, the average of all indices in the specified area on all days that meet the specified condition is obtained and a time series is created with this data set. The data set will be used in many statistical studies under certain standards in the continuation of the analysis and this study also facilitates working with long data. This study did not include a direct comparison between the calculated water quality indices and ground observations due to the unavailability of sufficient and spatially compatible in-situ data. Most available ground-based measurements are limited in both frequency and spatial coverage, often representing only single-point observations. In contrast, this study employs a spatially continuous analysis using satellite imagery, which makes direct comparison methodologically challenging and potentially misleading. Despite this limitation, the study relied on threshold values that are widely accepted in the literature and found that the spatial patterns and trends observed were in general agreement with the outcomes of previous ground-based research.

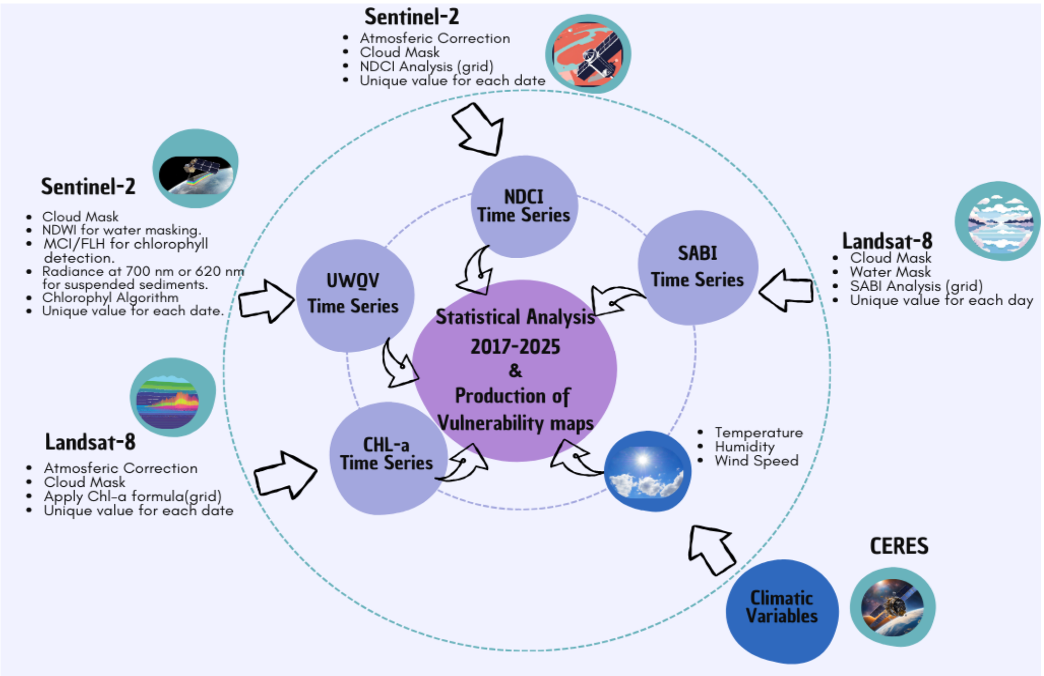

Figure 5. Schematic illustration of the methodology used for the analysis

5. Results and Discussion

As described in the methodology, the average of all indices in the specified area calculated from the images downloaded and analyzed for the period of 2017-2025 those meet the specified conditions. Time variation of Chl-a concentrations, NDCI, UWQV with SABI indices averaged for the study area are given in Figures 6, 7 and 8 respectively. Figure 6 shows that while the average Chl-a concentration is 2.66 mg/L, it exceeds 10 mg/L during the summer months. This increase corresponds with lower SABI index values (below -0.15), which generally remain above -0.1 throughout the rest of the year. Figure 7 illustrates that while the average NDCI index values are ~0, it exceeds 0.1 during the summer months. This increase once again corresponds with lower SABI index values (below -0.15). When the UWQV index values were plotted with respect to the SABI Index values averaged for the study area (Figure 8) a similar trend was observed. UWQV index values exceeded a certain limit of 0.3 (indicating high chlorophyll concentrations) for the specific dates observed in Figures 6 and 7. A closer look at the specific dates selected from the analysis (marked by red arrows in Figure 6) revealed that in the summers, mostly during August, the inner bay area becomes problematic in all of the years during the studied period.

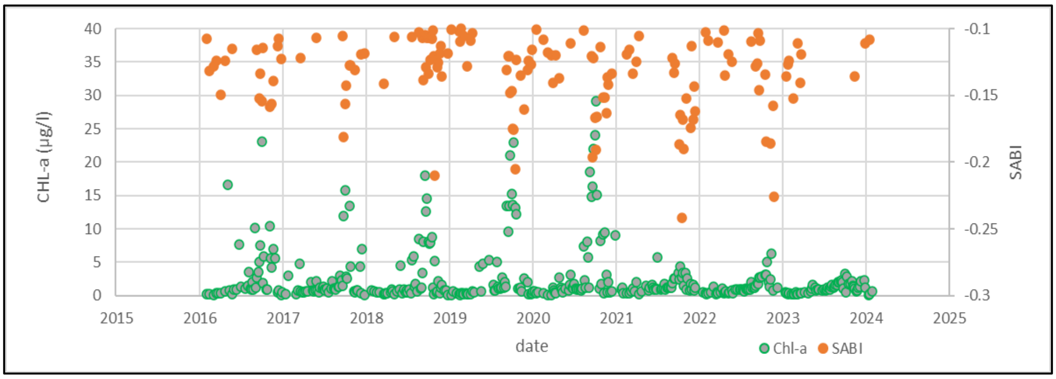

Figure 6. Temporal variation of the averaged Chl-a concentrations compared to the averaged SABI index values across the study area.

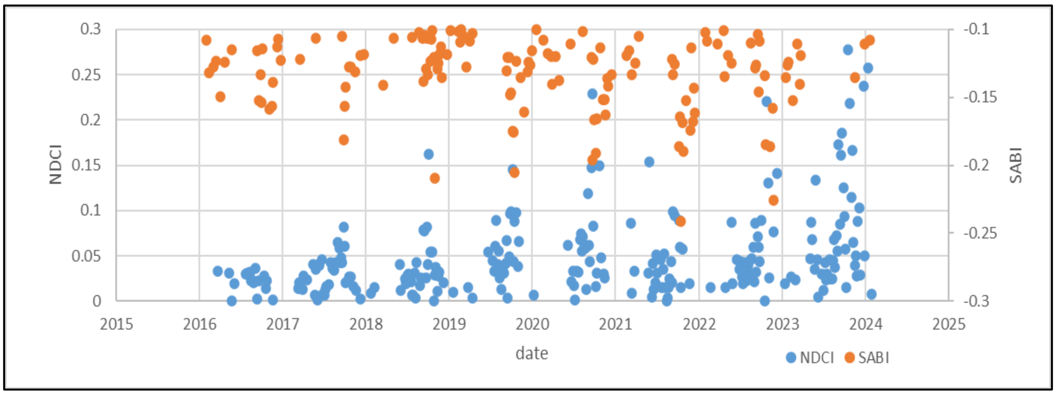

Figure 7. Temporal variation of the averaged NDCI index values compared to the averaged SABI index values across the study area

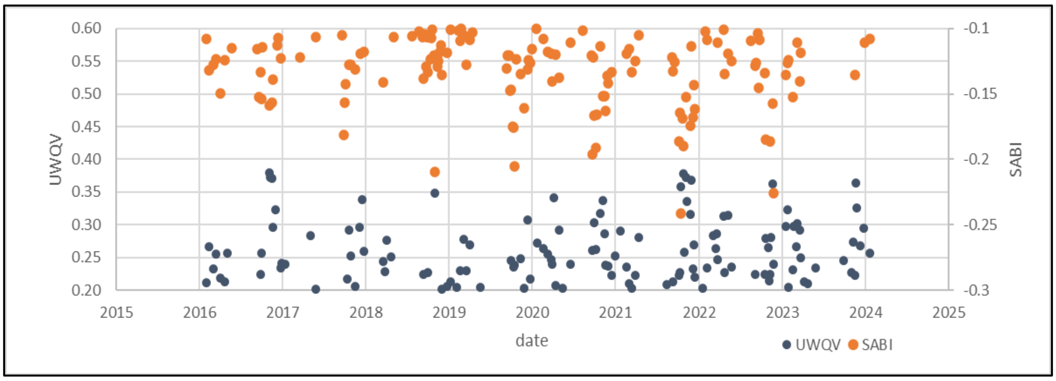

Figure 8. Temporal variation of the averaged UWQV index values compared to the averaged SABI index values across the study area.

Figure 9 shows the temporal variation of the TSI values averaged across the study area and indicates that the inner bay area reaches eutrophic/hypertrophic status especially in summer time. Based on evaluation of all water quality indicators, we selected the most problematic dates (21Aug2017, 26Aug2018, 13Aug2019, 09Sep2020, 04Sep2021, 24Sep2023 and 19Aug2024) and presented the NDCI and SABI water quality index maps in Figure 10 and Figure 11 respectively.

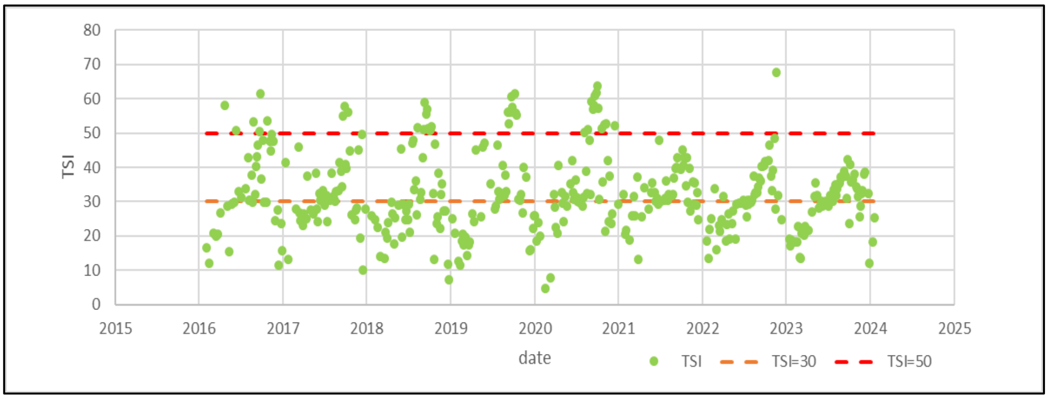

Figure 9. Temporal variation of the TSI values averaged across the study area

The spatial distribution of NDCI and SABI values reveals that the highest concentrations are observed near the mouths of streams discharging into the bay. These areas, which are greatly affected by sediment transport and nutrient flow, serve as hotspots for algal activity and organic matter accumulation. Figures 10 and 11 show the changes in NDCI and SABI values over multiple years, highlighting the persistence of these high concentration zones.

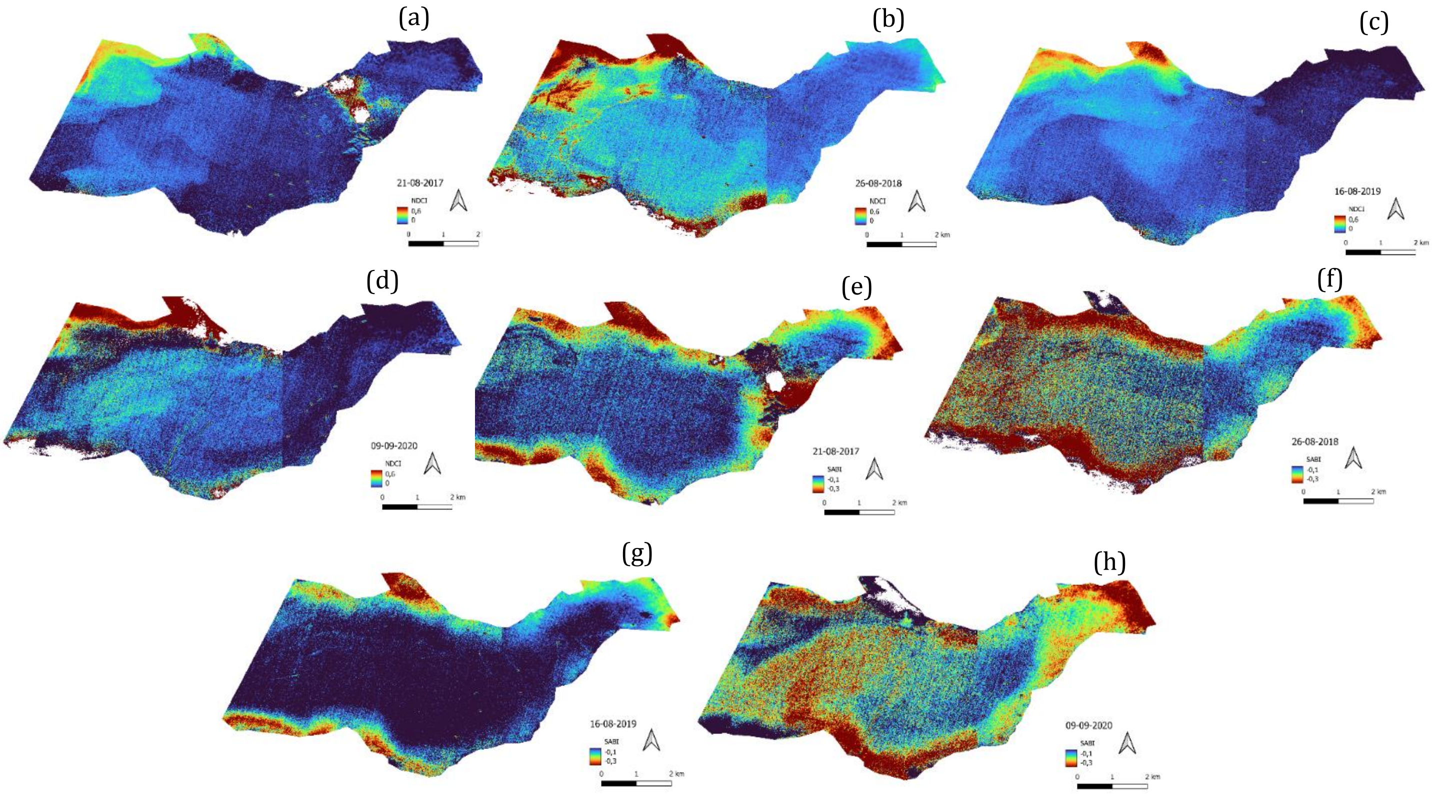

Figure 10. Comparison of NDCI values and SABI values estimated on (a) 21Aug2017, (b) 26Aug2018, (c) 13Aug2019, (d) 09Sep2020 (NDCI) and (e) 21Aug2017, (f) 26Aug2018, (g) 13Aug2019, (h) 09Sep2020 (SABI)

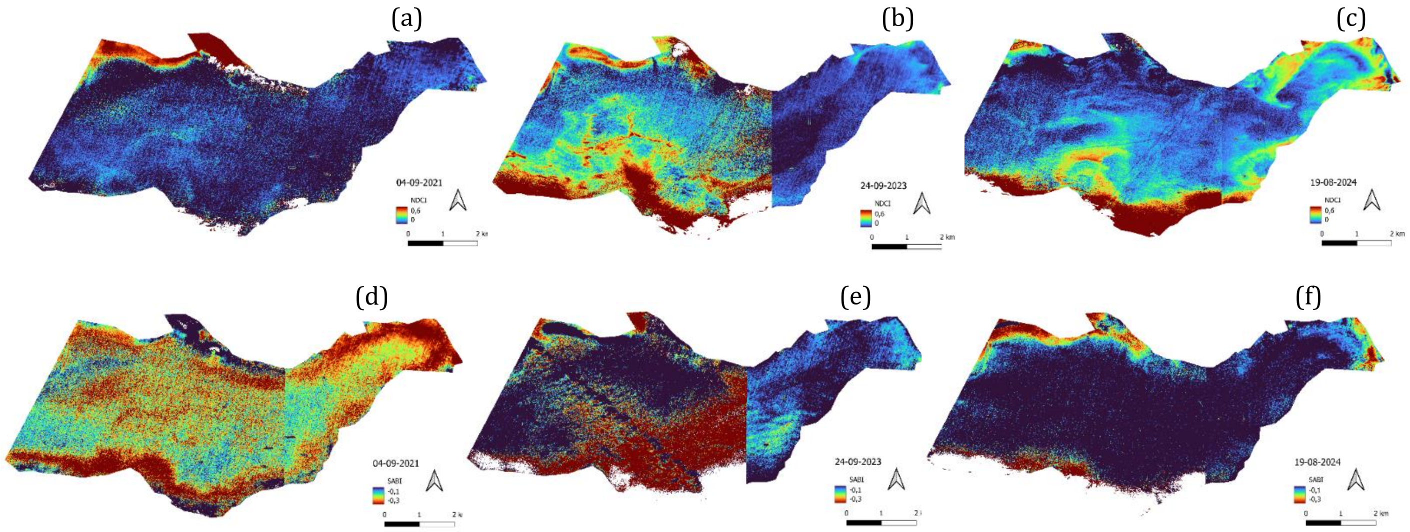

Figure 11. Comparison of NDCI values and SABI values estimated on (a) 04Sep2021, (b) 24Sep2023, (c) 19Aug2024 (NDCI) and (d) 04Sep2021, (e) 24Sep2023, (f) 19Aug2024 (SABI)

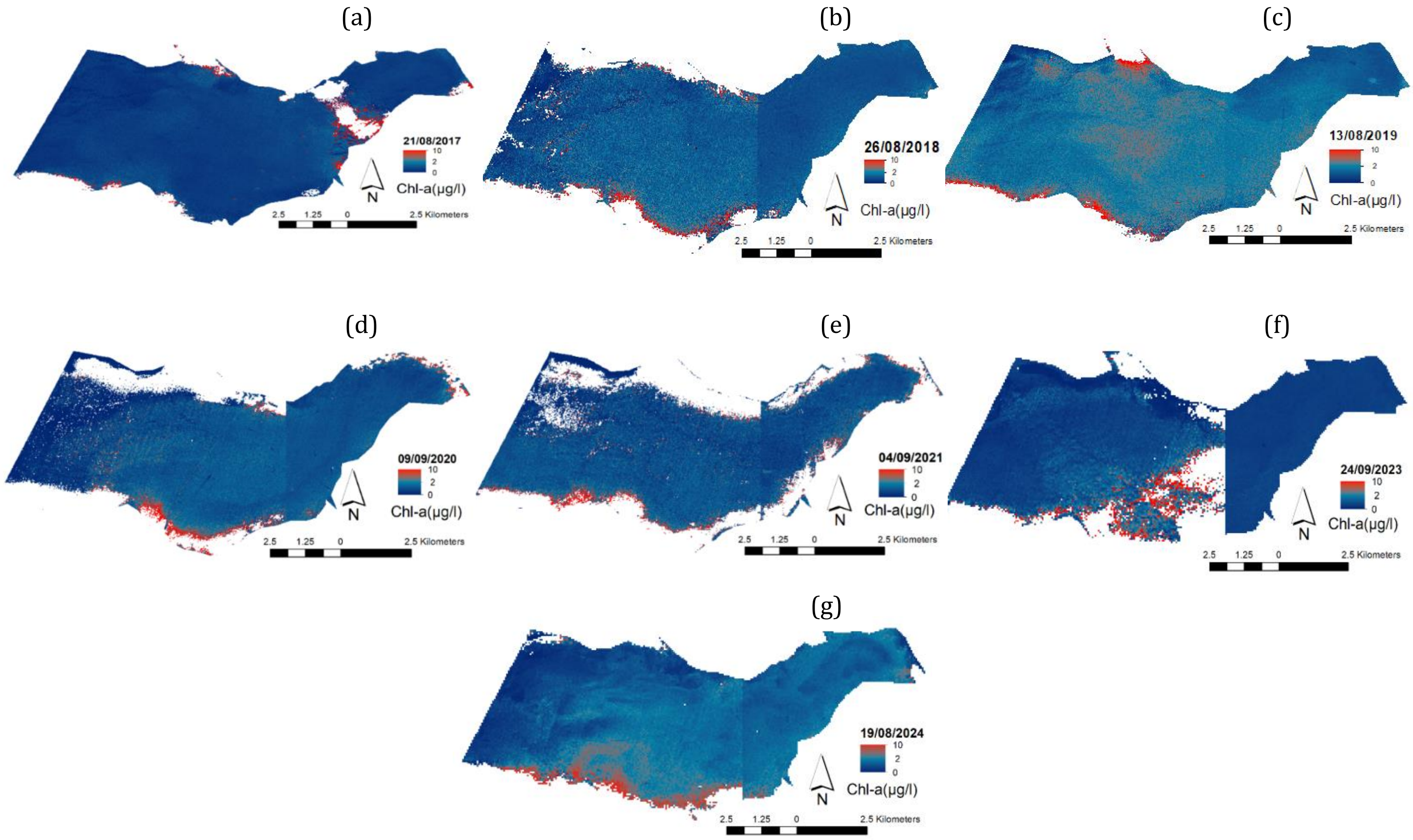

Figure 12. Chl-a concentrations estimated on (a) 21Aug2017, (b) 26Aug2018, (c) 13Aug2019, (d) 09Sep2020, (e) 04Sep2021, (f) 24Sep2023 and (g) 19Aug2024

It is even more evident in Figure 12 that, the areas with the high Chl-a concentrations coincide where Poligon, Ilıca streams in the south and Bostanlı and Çiğli streams in the north discharge into the bay pointing out the nutrient transfer from the streams to the inner bay. Figure 12 suggest that alluvial deposits and sediments carried by streams, along with possibly untreated domestic and industrial wastewater, contribute to nutrient enrichment in the inner bay, leading to elevated chlorophyll-a concentrations.

5.1. Results of the correlation analysis among water quality indices and climatic parameters

Key correlations among water quality indices and climatic parameters are provided in Table 2. In summary; NDCI shows a strong positive correlation with air temperature, particularly in the Spearman's rank correlation (rs = 0.67), indicating a significant relationship between these parameters. It also has a moderate negative correlation with UWQV (rs = -0.51) and relative humidity (rs = -0.46), suggesting that higher air temperatures and lower relative humidity levels may influence NDCI positively. CHL-a is most strongly positively correlated with air temperature across all correlation methods, with the highest being Spearman's rank (rs = 0.62). This suggests that Chl-a concentrations increase with rising air temperatures. Additionally, it has a moderate negative correlation with relative humidity (rs = -0.6), implying an inverse relationship.

SABI exhibits a significant negative correlation with UWQV (rs = -0.55) and a weak positive correlation with air temperature (rs = 0.08). These results indicate that SABI decreases as UWQV values increase. UWQV has a moderate negative correlation with air temperature (rs = -0.42) and a weak positive correlation with relative humidity (rs = 0.26). This reflects the influence of temperature and moisture on water quality variation. Air temperature has a strong negative correlation with relative humidity (rs = -0.82), highlighting the expected inverse relationship between these climatic parameters. Wind speed does not show strong correlations with other parameters, although it has a weak positive correlation with CHL-a (rs = 0.23) and air temperature (rs = 0.15). Overall, air temperature emerges as a key parameter, strongly correlated with both biological indices like CHL-a and NDCI, as well as climatic variables like relative humidity.

In addition to average values, the standard deviation (SD), minimum, and maximum values were calculated to better understand the temporal variability. For example, the Chl-a concentration had an average of 2.66 mg/L, with a standard deviation of 4.68 mg/L, ranging from 0.07 mg/L to 44 mg/L. Similarly, NDCI values ranged from -0.24 to 0.44 (mean ≈ 0.01, SD = 0.08), and SABI values ranged from -0.24 to 0.21 (mean = -0.07, SD = 0.06). These indicate significant seasonal anomalies, especially in late summer months.

Spearman's rank correlation coefficient is selected for discussion due to the non-parametric nature of the data and the possibility of non-linear relationships between climatic parameters and water quality indices. When analyzed seasonally, the correlation between Chl-a and temperature was found to be strongest during July–September (rs = 0.72), while it weakened significantly in winter months (rs = 0.35). Similarly, the inverse relationship between relative humidity and NDCI was most pronounced in August and September, reflecting peak algal bloom periods. These results emphasize the importance of seasonal variability in understanding climatic influence on algal indicators.

Table 2. Correlation matrix among water quality indices and climatic parameters

	NDCI	CHL-a	SABI	UWQV	Air Temp	Rel. Hum	Wind spd.	
NDCI	1.00	0.30	0.21	-0.38	0.47	-0.31	-0.01	Kendall tau
	1.00	0.24	0.21	-0.48	0.56	-0.37	-0.07	Pearson' r
	1.00	0.41	0.27	-0.51	0.67	-0.46	-0.01	Spearman's rs
CHL-a	0.30	1.00	-0.06	0.03	0.44	-0.42	0.16	
	0.20	1.00	-0.36	0.20	0.31	-0.29	0.12	
	0.41	1.00	-0.11	0.04	0.62	-0.60	0.23	
SABI	0.21	-0.06	1.00	-0.45	0.05	-0.02	-0.02	
	0.21	-0.36	1.00	-0.55	0.07	-0.03	-0.04	
	0.27	-0.11	1.00	-0.55	0.08	-0.03	-0.03	
UWQV	-0.38	0.03	-0.45	1.00	-0.28	0.18	0.02	
	-0.48	0.20	-0.55	1.00	-0.39	0.24	0.07	
	-0.51	0.04	-0.55	1.00	-0.42	0.26	0.03	
Air Temp.	0.47	0.44	0.05	-0.28	1.00	-0.61	0.11	
	0.56	0.31	0.07	-0.39	1.00	-0.79	0.08	
	0.67	0.62	0.08	-0.42	1.00	-0.82	0.15	
Rel. Hum.	-0.31	-0.42	-0.02	0.18	-0.61	1.00	-0.12	
	-0.37	-0.29	-0.03	0.24	-0.79	1.00	-0.14	
	-0.46	-0.60	-0.03	0.26	-0.82	1.00	-0.17	
Wind spd.	-0.01	0.56	-0.02	0.02	0.11	-0.12	1.00	
	-0.07	0.12	-0.04	0.07	0.08	-0.14	1.00	
	-0.01	0.23	-0.03	0.03	0.15	-0.17	1.00	

5.2. Vulnerability maps

The areas posing high risks are determined spatially by the analysis of water quality indices for the selected dates determined from the time series of averaged index values for the inner bay area (Figure 6). By overlaying the water quality index maps based on the selected filters (i.e., NDCI is greater than 0; -0.3<SABI<-0.1 and Chl-a concentrations are greater than 2) demonstrating hotspots, the vulnerability maps are produced for the selected dates (Figure 13). The thresholds used for generating vulnerability maps were based on literature and empirical observation. For instance, NDCI > 0 has been previously associated with increased cyanobacterial activity (e.g., Mishra & Mishra, 2012), while SABI values between -0.3 and -0.1 indicate high algal content with low surface reflectance due to bloom presence (Alawadi, 2010). A Chl-a concentration threshold of 2 mg/L was selected based on OECD eutrophication standards, marking the transition from mesotrophic to eutrophic conditions in freshwater systems.

In Figure 13, when all the filtering conditions are met, a value of 1 is assigned; otherwise, value of 0 is given. A final map is then produced based on overlaying of these vulnerability maps produced for the most critical conditions observed in the inner bay for the duration of the study period. As can be seen in Figure 14, the areas posing highest vulnerability coincide where Poligon, Ilıca streams in the south and Bostanlı and Çiğli streams in the north discharge into the bay. The results highlight that for any planned external intervention method with the algal blooms, the mitigation strategies should involve rehabilitation of these areas presented by this study.

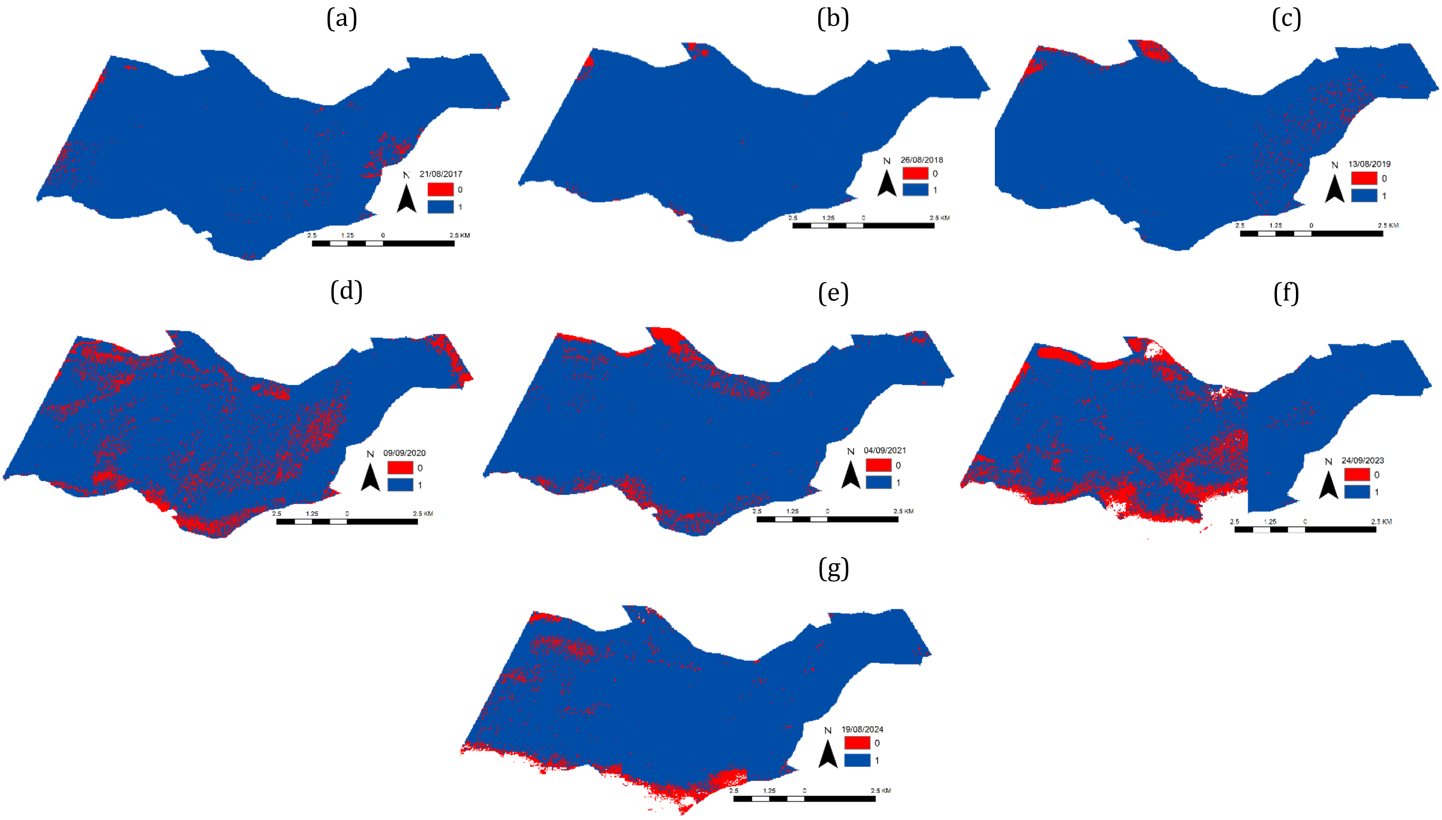

Figure 13. Vulnerability maps produced by overlaying indices on selected dates of on (a) 21Aug2017, (b) 26Aug2018, (c) 13Aug2019, (d) 09Sep2020, (e) 04Sep2021, (f) 24Sep2023 and (g) 19Aug2024

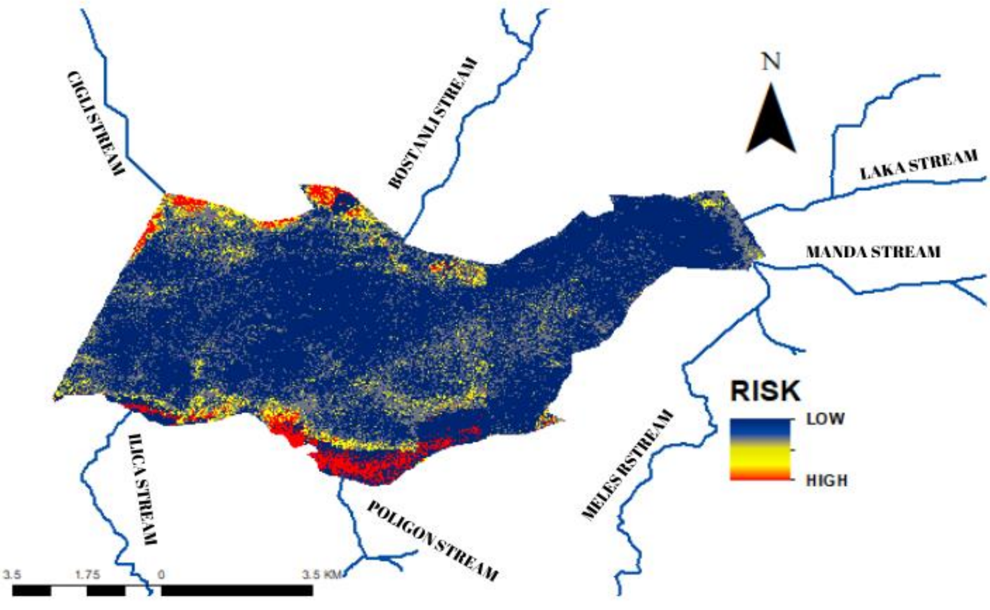

Figure 14. Overlayed vulnerability map for the inner bay of Izmir

6. Conclusion

This study highlights the link between frequently observed algal blooms, fish mortality, and foul odors in the inner İzmir Bay during the summer, emphasizing the impacts of human activities on aquatic ecosystems. The findings provide valuable insights into the impacts of climate change and human activities on coastal ecosystems, contributing to the development of targeted management and mitigation strategies.

The study demonstrates that an approach integrating water quality indices (i.e. NDCI, SABI and UWQV) estimating with real-time satellite data can be used as early-warning systems to alert stakeholders and can support taking proactive measures when water quality thresholds are exceeded. Such systems, coupled with meteorological data monitoring will empower decision-makers to respond promptly to worsening water conditions. As climate challenges intensify, remote sensing stands as a vital tool for safeguarding water resources, offering smarter, more sustainable solutions for water quality management.

This study quantified and compared the water quality indices (NDCI, SABI and UWQV) and the estimated Chl-a concentrations with the climatic variables for the whole inner bay using the longest available data for the period of 2017-2025. Not surprisingly, correlation analysis showed that estimated aerial averaged NDCI index and Chl-a concentration values show a strong positive correlation with air temperature, particularly in the Spearman's rank correlation (r_s = 0.67 and 0.62 respectively), indicating a significant relationship between these parameters.

Unlike other studies that utilized Google Earth Engine for estimation of indices and Chl-a concentrations, we developed a customized code using Python to independently download and analyze raw satellite data with respect to defined corrections/masks (available as Data Supplement).

This is the first comprehensive study conducted for İzmir Bay, seeking relationships between the water quality indices and the climatic variables to explain the environmental disaster observed in the bay area. The results of the study point out how the bay area becomes vulnerable especially where Poligon, Ilıca streams in the south and Bostanlı and Çiğli streams in the north discharge into the bay. It is recommended to consider these high risk areas primarily when mitigation strategies are considered for the area.

Although this study sheds light on the deterioration of water quality by comparing water quality indices with meteorological data and identifying the inner bay's vulnerable zones, it does not take a hydrobiologist's perspective into account. The possibility that fish deaths may have resulted in the inner bay of Izmir, in summer 2024, from the proliferation of predatory cyanobacteria in the aquatic ecosystem, has not been considered/studied in this study. While this remains a potential factor, the current study highlights that water quality significantly deteriorates every summer, raising an alarm. It also demonstrates that similar issues could lead to disastrous outcomes if the balance in the aquatic ecosystem shifts even slightly.

However, the lack of in situ hydrobiological sampling is a limitation in this study, as it prevents direct validation of satellite-based estimates. Future studies should include simultaneous field observations to strengthen the ecological interpretation of satellite data and to more comprehensively assess fish mortality due to algal blooms.

Author Contributions:
A. A. Erdem: Conceptualization, Writing—original draft, Formal analysis.
H. Sekerci: Data Curation, Formal analysis.
H. S. Elçi: Conceptualization, Writing—original Draft, Writing—review, editing and Supervision.

Research and publication ethics statement: In the study, the authors declare that there is no violation of research and publication ethics and that the study does not require ethics committee approval.

Conflicts of Interest: The authors declare no conflicts of interest.

References

Aktaş, N., Demir, F., & Özkan, Z. (2022). The water quality of Izmir Bay: A Case Study. *Environmental Monitoring and Assessment*, 194(5), 312–324.

Anadolu Agency. (2024). İzmir Körfezi'nde balık ölümleri devam ediyor (in Turkish). Retrieved January, 31, 2024 from https://www.denizbulten.com/izmir-korfezinde-balik-olumleri-devam-ediyor-55449h.htm

Aegean Sea Water Quality Report. (2022). Water quality bulletin published as a part of the monitoring program conducted by the Turkish Ministry of Environment, Urbanization and Climate.

Alharbi, M. (2023). Spectral indices for monitoring algal bloom dynamics in the red sea coast between Jeddah and Rabigh. *Marine Pollution Bulletin,* 187, 114574. https://doi.org/10.1016/j.rsase.2023.100935

Alawadi, F. (2010). Development of the surface algal bloom index (SABI) for assessing submerged aquatic vegetation. *Environmental Monitoring and Assessment,* 168(1), 511–524. https://doi.org/10.1117/12.862096

Beutel, M. W., & Horne, A. J. (2009). A review of the effects of hypolimnetic oxygenation on lake and reservoir water quality. *Lake and Reservoir Management,* 15(4), 285–297. https://doi.org/10.1080/07438149909354124

Braaten, J., Cohen, J., & Yang, X. (2015). Cloud detection algorithm for satellite-based water quality monitoring. *Remote Sensing of Environment,* 160, 171–182.

Carlson, R. E. (1977). A trophic state index for lakes. *Limnology and Oceanography*, 22(2), 361–369. https://doi.org/10.4319/lo.1977.22.2.0361

Chawira, M., Dube, T., & Gumindoga, W. (2013). Remote sensing based water quality monitoring in Chivero and Manyame lakes of Zimbabwe. *Physics and Chemistry of the Earth, Parts A/B/C*, 66, 38–44. https://doi.org/10.1016/j.pce.2013.09.003

Chorus, I., & Welker, M. (2021). Toxic cyanobacteria in water: A guide to their public health consequences, monitoring and management. Taylor & Francis.

Davis, T. W., Berry, M. A., Boyer, G. L., & Gobler, C. J. (2019). The effects of nitrogen and phosphorus on cyanobacterial metabolism and toxin production. *Harmful Algae*, 81, 1–12.

El-Shehawy, R., Gorokhova, E., Fernández-Piñas, F., & del Campo, F. F. (2012). Global warming and harmful cyanobacteria blooms: What can be learned from experiments and field studies? *Water Research,* 46(5), 1347–1358. https://doi.org/10.1016/j.watres.2011.11.021

Gitelson, A. A., Gurlin, D., Moses, W. J., & Barrow, T. (2009). A bio-optical algorithm for the remote estimation of the chlorophyll-a concentration in case2 waters. *Environmental Research Letters,* 4(4), 045003. https://doi.org/10.1088/1748-9326/4/4/045003

Häder, D. P., & Gao, K. (2015). Interactions of anthropogenic stress factors on marine phytoplankton. *Frontiers in Environmental Science*, 3, 14. https://doi.org/10.3389/fenvs.2015.00014

Han, L., & Rundquist, D. C. (1997). Comparison of NIR/Red Ratio and first derivative of reflectance in estimating algal-chlorophyll concentration: A case study in a turbid reservoir. *Remote Sensing of Environment*, 62(3), 253–261. https://doi.org/10.1016/S0034-4257(97)00106-5

Hansen, J., & Williams, D. (2018). Satellite-based chlorophyll-a monitoring in dynamic coastal waters: Applications and challenges. *Journal of Environmental Monitoring*, 20(5), 1124–1132.

Hollstein, A., Fischer, J., Preusker, R., Finkensieper, S., & Dinter, T. (2016). Neural network cloud detection for Sentinel-2 MSI data. *Remote Sensing of Environment,* 178, 277–290.

McFeeters, S. K. (1996). The use of the Normalized Difference Water Index (NDWI) in the delineation of open water features. *International Journal of Remote Sensing,* 17(7), 1425–1432. https://doi.org/10.1080/01431169608948714

Mishra, S., & Mishra, D. R. (2012). Normalized Difference Chlorophyll Index: A novel model for remote estimation of chlorophyll-a concentration in turbid productive waters. *Remote Sensing of Environment*, 117, 394–406. https://doi.org/10.1016/j.rse.2011.10.016

Ndungu, L. W., Ndiritu, G. G., & Mutua, B. M. (2013). Remote sensing for water quality monitoring in Lake Victoria. *African Journal of Science, Technology, Innovation and Development, 5*(5), 399–409.

Paerl, H. W., & Huisman, J. (2008). Climate change: A catalyst for global expansion of harmful cyanobacterial blooms. *Environmental Microbiology Reports*, 1(1), 27–37. https://doi.org/10.1111/j.1758-2229.2008.00004.x

SSEC. (2012). Space Science and Engineering Center (SSEC) Retrieved January, 31, 2024 from https://www.ssec.wisc.edu

Thiemann, S., & Kaufmann, H. (2002). Lake water quality monitoring using hyperspectral airborne data—a semi-empirical multisensor approach. *Remote Sensing of Environment*, 81(3), 228–237. https://doi.org/10.1016/S0034-4257(01)00345-5

TMMOB. (2024) Chamber of Environmental Engineers İzmir Branch Water Report. Retrieved January, 31, 2024 https://icerik.cmo.org.tr/uploads/ContentFiles/2024-22-3-12-15-16-484547.pdf

Tuygun, G. T., Salgut, S., & Elçi, A. (2023). Long-term spatial-temporal monitoring of eutrophication in Lake Burdur using remote sensing data. *Water Science & Technology*, 87(9), 2184. https://doi.org/10.2166/wst.2023.113

Zhang, Y., Qin, B., Zhu, G., Zhang, J., & Gao, G. (2020). Variability and drivers of phytoplankton blooms in a large eutrophic lake observed using remote sensing. *Water Research*, 170, 115312.

Zlinszky, A., & Padányi-Gulyás, G. (2020). Ulyssys water quality viewer: A satellite-based global near real time water quality visualization. Proceedings Book of EGU General Assembly. Online. https://doi.org/10.5194/egusphere-egu2020-18256